International Journal of Minerals, Metallurgy and Materials
Accepted manuscript, https://doi.org/10.1007/s12613-020-2015-2

Roasting and water leaching behavior of zinc in zinc oxidized ore using $(NH_4)_2SO_4$

Xiao-yi Shen[1)] , *Hong-mei Shao*[2)], *Ji-wen Ding*[3)], *Yan Liu*[1)], *Hui-min Gu*[1)], *and Yu-chun Zhai*[1)]

1) School of Metallurgy, Northeastern University, Shenyang 110819, China.

2) School of Environmental and Chemical Engineering, Shenyang Ligong University, Shenyang 110159, China.

3) School of Computer Science and Engineering, Northeastern University, Shenyang 110819, China.

Abstract: An improved method of $(NH_4)_2SO_4$ roasting followed by water leaching to utilize zinc oxidized ore was studied. The operating parameters were obtained by investigating the influences of the molar ratio of $(NH_4)_2SO_4$ to zinc, roasting temperature and holding time on zinc extraction. The roasting process followed the chemical reaction control mechanism with the apparent activation energy value of 41.74 kJ·mol^{-1}. The transformation of mineral phases in roasting was identified by XRD analysis combining with TG-DTA curves. The water leaching conditions including leaching temperature, time, stirring velocity and liquid-solid ratio were discussed and the leaching kinetics was also studied. The reaction rate was under the outer diffusion of no product layer control with the values of the apparent activation energy for two stages of 4.12 kJ·mol^{-1} and 8.19 kJ·mol^{-1}, respectively. The maximum zinc extraction ratio reached 96%, while the extraction efficiency of iron was about 32% at the appropriate conditions. The work offers an effective method that zinc oxidized ore can be comprehensive used.

Key words: zinc oxidized ore; $(NH_4)_2SO_4$ roasting, water leaching; kinetics; mechanism; extraction ratio

1. Introduction

Zinc is one of the important nonferrous metals and is extensively applied in galvanization, alloy, battery and other fields. For a long time, sulfide ores have been the main raw material in zinc metallurgy [1-2]. However, due to the overexploitation of sulfide ores and the increased zinc demand, much attention has been paid to the reasonable exploitation of zinc oxidized ores [2-9].

As the largest resources bearing zinc [4-5,10], zinc oxidized ores usually exist as

Corresponding author: Xiao-yi Shen E-mail: shenxy@smm.neu.edu.cn

oxidized carbonate or silicate minerals, for instance, smithsonite ($ZnCO_3$), willemite ($ZnSiO_4$), hemimorphite ($Zn_4Si_2O_7(OH)_2 \cdot H_2O$) etc. [4,11-14] and usually contain a high grade silica [7,15]. To date, extensive studies have been carried out in treating zinc oxidized ores. It is difficult to concentrate zinc oxidized ores by flotation because to its fine intergrowth, complex phase compositions and high gangue content [3,16-17]. Both pyrometallurgical and hydrometallurgical routes are adopted to utilize the zinc oxidized ores. Among them, the traditional pyrometallurgical processes have no competitiveness because of high energy consumption and high CO_2 and residue emissions [17-21]. Generally, the hydrometallurgical routes are divided into acid leaching and alkaline leaching, which includes ammonia leaching and sodium hydroxide leaching. The sulfuric acid leaching is wildly applied and is found to be versatile [19,22]. But the production parameters have to be properly controlled in sulfuric acid leaching, or silica gel is inevitably formed, making the filtration difficulty [6-7,23-24]. Many efforts have been done to improve the filtration performance by precipitating silica, comprising of the control of pH value [25-26], the adding flocculating agent [12,26], the addition of Al^{3+} [11,24,27] and so on. Ammonia leaching has high efficiency in treating zinc oxidized ores for the formation of stable zinc ammine complexe [2,9,12,26]. It is noteworthy that the leaching vessels need to be hermetically sealed to avoid the ammonia volatilization [3,17,28]. Sodium hydroxide leaching is also a promising route and many reports have been published referring to alkaline treatment of zinc-bearing minerals. But the decomposition of willemite and hemimorphite is slow [7,29-31], and additional work is needed to realize the separation of Zn, Si and Pb [7,32]. Bioleaching is also carried out but there is still a certain distance to realize industrialization [33]. In metallurgy, as a strong acid and weak base salt, ammonium sulfate gets a lot of attention and is frequently applied for the extraction of valuable metals from various low-grade ores, including zinc oxidized ore, wollastonite, blast furnace slag and so on [10,34-37]. To realize the comprehensive utilization of zinc oxidized ore, an improved and effective process was developed. First, the mixture of zinc oxidized ore and $(NH_4)_2SO_4$ was roasted. After water-leaching and filtration, zinc and small amounts of iron entered into the filtrate and separated from silica and calcium that remained in leaching residue. The roasting gas absorbed by dilute H_2SO_4 or water was transformed into $(NH_4)_2SO_4$ or ammonia water [17]. Second, the leaching solution was used to prepare zinc products after purification and iron was utilized subsequently. Third, the enriched strontium and lead

in leaching residue were recovered through a conversion method. Fourth, silica was extracted and used to prepare white carbon black, fibrous xonotlite and stereo-porous tobermorite. Finally, the remaining residue was used to recover iron. In the whole process, the valuable components including Zn, Si, Pb, Sr and Fe are extracted and made into products. Water, $(NH_4)_2SO_4$ and NaOH are cycled. The detailed process flow chart is shown in Fig. 1.

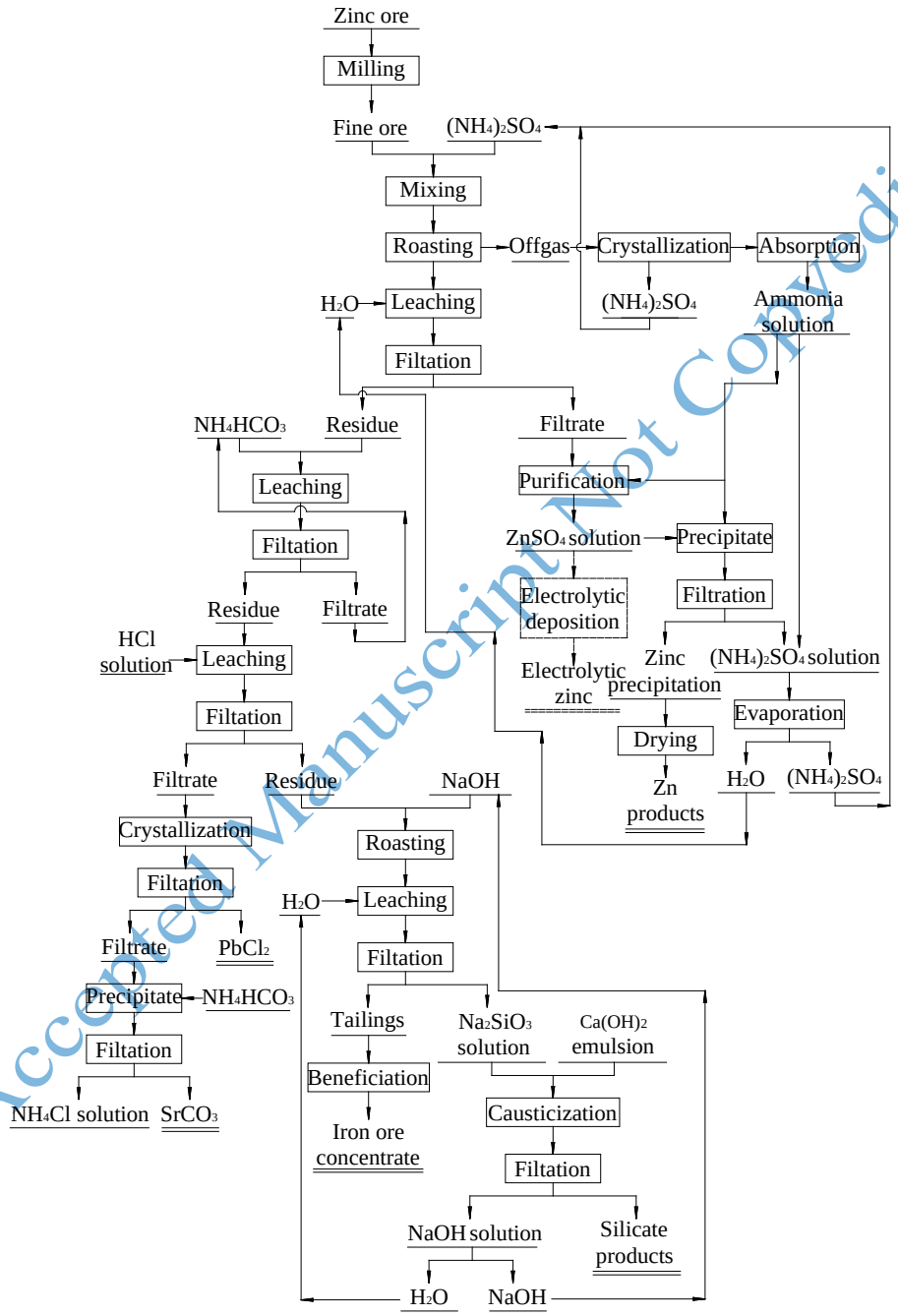

Fig. 1. Process flow chart of comprehensive utilization of zinc oxidized ore

In this investigation, a typical zinc oxidized ore from Lanping located in southwest

of China was used as raw material, which was roasted by industrial $(NH_4)_2SO_4$ followed by water leaching. The influences of molar ratio of $(NH_4)_2SO_4$ to zinc, reaction temperature and holding time on the extractions of zinc and iron were determined. The transformation of mineral phases was identified by XRD and TG-DTA analysis. Moreover, the water leaching temperature, time, stirring velocity and liquid-solid (L/S) ratio on the leaching ratio of zinc were discussed. At last, the roasting mechanism and water leaching kinetics were determined using the constant conversion method and shrinking core model, respectively.

2. Experimental

2.1. Materials

The zinc oxidized ore with the particle size below 74 μm was used as raw material. Industrial grade $(NH_4)_2SO_4$ was used as reactant as received.

2.2. Procedure

A resistance furnace (temperature accuracy ±1ºC) was employed in roasting experiments. 50 grams of powder-like zinc oxidized ore and a specific amount of $(NH_4)_2SO_4$ were uniformly mixed and put in a crucible that was then placed in the furnace. After the temperature reached the specified value ranging from 300ºC to 500ºC and maintained a period of time within 2.5 h, the sample was taken out and leached in water at 80ºC for 1 h with a liquid-solid ratio of 4:1. For kinetic analysis, once the temperature reached the required value, the mixtures were removed within a predesigned time interval of 10 min and cooled rapidly.

The leaching investigation was conducted at a certain L/S ratio from 2:1 to 6:1. The vessel containing distilled water in a waterbath was continuously stirred. Once the temperature rose to the desired value from 20ºC to 95ºC and stabilized, the samples were added into the vessel and leached for a period of time under stirring. Then the slurry was filtrated before analysis. For kinetic analysis, the specimens were collected at selected time intervals of 5 min, filtered and determined using EDTA titration.

The extraction ratio of Zn was determined using Eq. 1 as following.

$$\eta = \frac{V \times c}{\mathrm{G} \times \mathrm{w}} \times 100\% \quad (1)$$

where η is the extraction ratio of Zn, %; V is the volume of leaching solution, L; c is the zinc concentration, $g \cdot L^{-1}$; G is the weight of zinc oxidized ore, g; w is the level of Zn in zinc oxidized ore, %.

3. Results and discussion

3.1. Analysis of zinc oxidized ore

The main compositions of the zinc oxidized ore analyzed by chemical method were listed in Table 1. The powder-like ore was characterized by XRD and SEM, as shown in Fig. 2. As one of the main compositions, the content of ZnO is 29.12%, mainly existing as $ZnCO_3$ and Zn_2SiO_4. The contents of PbO and SrO are 3.66% and 1.81%, respectively. Others are iron oxide, SiO_2 and CaO in the grades of 9.02%, 27.85% and 2.50%. The XRD study indicates smithsonite and quartz exist as the major mineral phases and $CaCO_3$, $PbCO_3$, $CaSO_4 \cdot 2H_2O$, Fe_2O_3 and Zn_2SiO_4 as the minor phases. The zinc oxidized ore particles are uneven and irregular.

Table 1. Main chemical compositions of the zinc oxidized ore **wt/%**

Components	ZnO	Fe_2O_3	SiO_2	PbO	SrO	CaO
Content / wt%	29.12	9.02	27.85	3.66	1.81	2.50

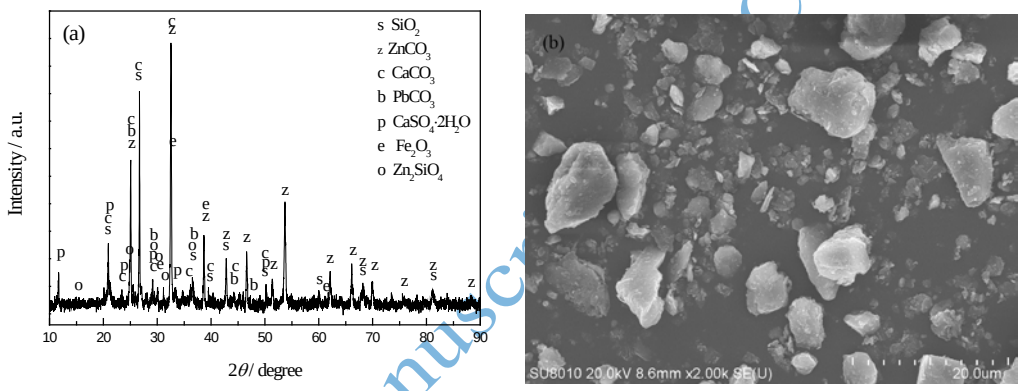

Fig. 2. (a) XRD pattern and (b) SEM micrograph of the zinc oxidized ore.

3.2. Roasting mechanism

The experiments were implemented to examine the influence of molar ratio of $(NH_4)_2SO_4$ to zinc, reaction temperature and holding time on the extractions of zinc and iron at the particle size below 74 μm and the results were plotted in Fig. 3.

3.2.1. Influence of molar ratio of $(NH_4)_2SO_4$ to zinc

The influence of molar ratio of $(NH_4)_2SO_4$ to zinc in zinc oxidized ore ranging from 1.0:1 to 1.45:1 on the extractions of zinc and iron was discussed under conditions of 450ºC holding for 2 h, as displayed in Fig. 3(a). It shows that an increase in molar ratio has appreciable impact on the extractions of zinc and iron. Zinc extraction ratio increases from 74.38% at molar ratio of 1.0:1 to 94.99% at 1.4:1. The extraction ratio is close to that of pressure acid leaching reported by He et al. [24]. Afterwards, the

zinc extraction ratio has no obvious increase, but the iron extraction increases continuously. Sufficient $(NH_4)_2SO_4$ is necessary for obtaining a high zinc extraction ratio because the interaction between reactants is improved due to the improving contact area as increasing the dosage of $(NH_4)_2SO_4$. But more $(NH_4)_2SO_4$ results in not only excess consumption of auxiliary material, but also a high reaction ratio of iron. The molar ratio 1.4 was chosen.

3.2.2. Influence of reaction temperature

The study for the influence of roasting temperature ranging from 300ºC to 500ºC on the extractions of zinc and iron was performed under conditions of molar ratio 1.4:1 and holding time 2 h. The data shown in Fig. 3(b) reveals that the roasting temperature has an important impact in roasting process. Zinc extraction ratio increases from 10.09% at 300ºC up to 94.99% at 450ºC. But the variation is slight over 450ºC. It means that the temperature 450ºC is appropriate for extracting zinc. Furthermore, the extraction ratio of iron exhibits continuous increase. Increasing temperature promotes the reaction. The main reason is $(NH_4)_2SO_4$ is first decomposed into NH_4HSO_4 and NH_3 and then into $(NH_4)_2S_2O_7$, and even into N_2, SO_2 and NH_3 [38-42]. The reaction is transformed from solid-solid phase to liquid-solid phase in roasting temperature, which presumably decreases the reaction resistance [38-42].

3.2.3. Influence of holding time

The influence of holding time on the extractions of Zn and Fe was investigated under conditions of roasting temperature 450ºC and molar ratio 1.4:1. The extraction ratio of Zn in Fig. 3(c) increases obviously within 1 h, thereafter the change is inappreciable. The extraction ratio of Zn is 96.11% roasting for 1 h, while the extraction efficiency of Fe is 32.49%, implying the holding time of 1 h is enough for extracting Zn. The extraction ratio of Fe keeps increasing. Prolonging holding time increases the burden of eliminating iron and decreases the efficiency. From view point of reducing energy consumption, the holding time 1 h was chosen.

From the above, the appropriate roasting conditions could be concluded as below: reaction temperature of 450ºC, molar ratio of $(NH_4)_2SO_4$ to zinc in zinc oxidized ore of 1.4:1 and holding time of 1 h at particle size below 74 μm.

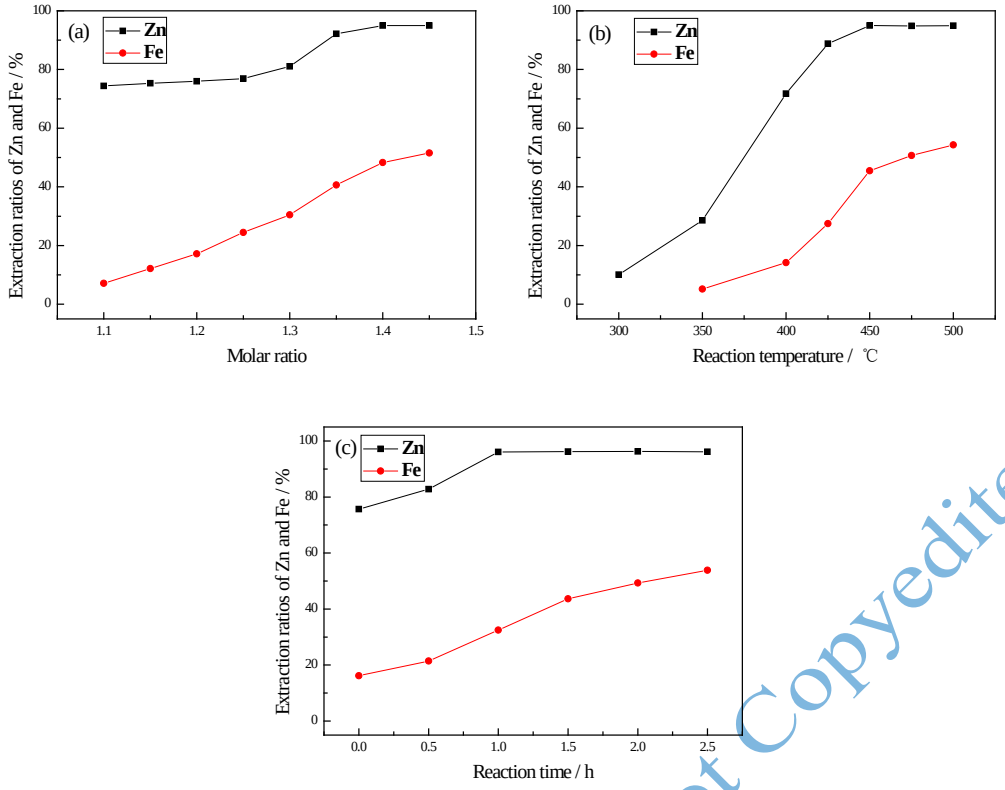

Fig .3. Influence of (a) molar ratio of $(NH_4)_2SO_4$ to zinc [450°C, 2 h]; (b) temperature [1.4:1, 2 h]; (c) holding time [450°C, 1.4:1] on the extraction ratios of Zn and Fe.

3.2.4. Analysis of roasting process

Fig. 4 shows the representative TG-DTA curves ranging from 25°C to 600°C of $(NH_4)_2SO_4$ and the mixture of zinc oxidized ore and $(NH_4)_2SO_4$ obtained at 10 $K \cdot min^{-1}$ of heating rate and 100 $mL \cdot min^{-1}$ of air flow rate. Three obvious endothermic peaks appear at approximate 310°C, 336°C and 435°C (Fig. 4(a)), accompanied by three prominent weight losses in TG curve at temperature ranges of 250-325°C with 12.80%, 325-350°C with 6.01% and 350-440°C with 80.77%. The weight loss of 12.80% and 6.01% are extremely close to the stoichiometric weight loss of losing a NH_3 from $(NH_4)_2SO_4$ and the formation of $(NH_4)_2S_2O_7$. The three endothermic peaks are assigned to the decomposition of $(NH_4)_2SO_4$, NH_4HSO_4 and $(NH_4)_2S_2O_7$, respectively according to the following reactions [38-39].

$$(NH_4)_2SO_4 \rightarrow NH_3 + NH_4HSO_4 \quad (1)$$

$$2NH_4HSO_4 \rightarrow (NH_4)_2S_2O_7 + H_2O \quad (2)$$

$$3(NH_4)_2S_2O_7 \rightarrow 2NH_3 + 2N_2 + 9H_2O + 6SO_2 \quad (3)$$

Five obvious endothermic peaks appear at approximate 65ºC, 205ºC, 302ºC, 335ºC and 420ºC (Fig. 4(b)), accompanied by three prominent weight losses in TG curve at temperature ranges of RT-280ºC with 11.16%, 280-320ºC with 12.81% and 320-440ºC with 21.51%. The first stage of weight loss is due to the dehydration and release of CO_2 from $ZnCO_3$. The second range is mainly attributed to $(NH_4)_2SO_4$ decomposition. The third one is extremely complex, comprising of the formations followed by deamination of $(NH_4)_2Zn(SO_4)_2$ and $(NH_4)_3Fe(SO_4)_3$, the formations of $CaSO_4$ and $PbSO_4$ and the total decomposition of $(NH_4)_2SO_4$ [38-40].

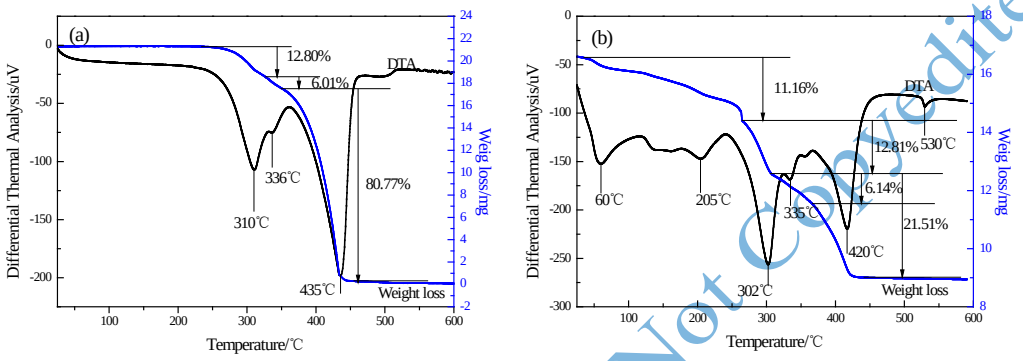

Fig. 4. TG-DTA curves of (a) $(NH_4)_2SO_4$ and (b) mixture of zinc ore and $(NH_4)_2SO_4$.

To illuminate the roasting process, XRD testing was adopted to identify the phase structures of the specimens obtained at different roasted temperatures, as presented in Fig. 5. Main phases in specimen obtained at 250ºC are almost the same as that of the initial mixture, indicating there is no substantial reaction occurring. Due to the strong diffraction peaks of $(NH_4)_2SO_4$, Zn_2SiO_4 and $PbCO_3$ are not detected. Main phases in 300ºC roasted specimen are $ZnCO_3$, SiO_2, $(NH_4)_2SO_4$, Zn_2SiO_4, $(NH_4)_2Zn(SO_4)_2$ and NH_4HSO_4. $(NH_4)_2Zn(SO_4)_2$ has been synthesized and the decomposition or reaction of $(NH_4)_2SO_4$ is incomplete. $ZnCO_3$ and $(NH_4)_2SO_4$ disappear in specimen obtained at 350ºC and $CaCO_3$ still remains stable, revealing the decomposition or reaction of $ZnCO_3$ has completed. $(NH_4)_3Fe(SO_4)_3$ has been formed at 350ºC from Fig. 5(b). Main phases in specimen obtained at 400 ºC are $CaSO_4$, SiO_2, $(NH_4)_2Zn(SO_4)_2$, $PbSO_4$, $CaCO_3$, $NH_4Fe(SO_4)_3$ and silicate, meaning that $CaSO_4$ and $PbSO_4$ have been formed and $NH_4Fe(SO_4)_2$ has been generated from $(NH_4)_3Fe(SO_4)_3$. Main phases in specimen obtained at 425ºC are SiO_2, $ZnSO_4$, $CaSO_4$, $(NH_4)_2Zn(SO_4)_2$, $PbSO_4$, $NH_4Fe(SO_4)_3$ and $Fe_2(SO_4)_3$. $ZnSO_4$ is assigned to $(NH_4)_2Zn(SO_4)_2$ decomposition.

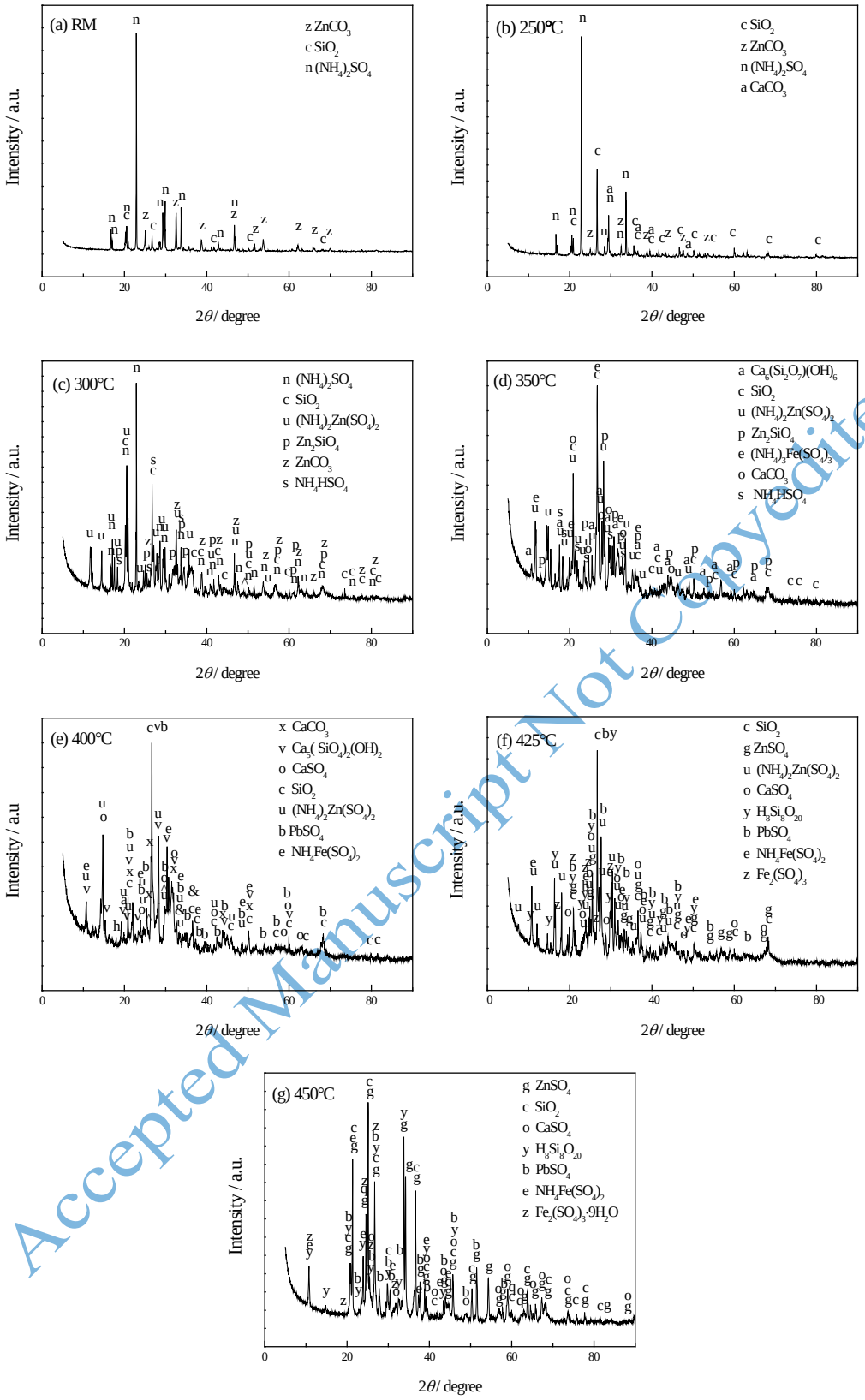

Fig. 5. XRD patterns of mixtures roasted at (a) RM; (b) 250°C; (c) 300°C; (d) 350°C; (e) 400°C; (f) 425°C; and (g) 450°C.

$CaCO_3$ disappears, revealing that the transformation to $CaSO_4$ has completed.

$Fe_2(SO_4)_3$ is generated from $NH_4Fe(SO_4)_2$. Main phases in sample obtained at 450ºC are similar with that of specimen obtained at 425ºC besides $(NH_4)_2Zn(SO_4)_2$ disappears and the intensity of the diffraction peaks of $ZnSO_4$ and $PbSO_4$ increase. $Fe_2(SO_4)_3 \cdot 9H_2O$ is attributed to the moisture absorption of roasting specimen. Quartz SiO_2 is stable throughout the whole roasting process. The diffraction peaks of NH_4HSO_4 are not conspicuous in Fig. 5(c) and (d), but NH_4HSO_4 was clearly identified as the decomposition product of $(NH_4)_2SO_4$ in some reports [34-37].

From above, the phases transformation in roasting process can be summarized as the following:

$ZnCO_3$ or ZnO decomposed transforms into $(NH_4)_2Zn(SO_4)_2$ at 300ºC, and further transforms into $ZnSO_4$ at 425ºC;

Fe_2O_3 transforms into $(NH_4)_3Fe(SO_4)_3$ at 350ºC, and further changes into $NH_4Fe(SO_4)_2$ at 400ºC and $Fe_2(SO_4)_3$ at 425-450ºC;

$PbSO_4$ and $CaSO_4$ are obtained when temperature reaches 400ºC.

Based on the XRD patterns and TG-DTA curves, the peak of TG-DTA curves at 302ºC is mainly caused by the decomposition of $(NH_4)_2SO_4$ and the formation of $(NH_4)_2Zn(SO_4)_2$. Sun et al. proved $(NH_4)_2SO_4$ began to decompose into NH_4HSO_4 when temperature exceeded 260ºC [17]. The peak at 335ºC is mainly assigned to the decomposition of NH_4HSO_4 and the formation of $(NH_4)_3Fe(SO_4)_3$. The peak at 420ºC is mainly assigned to the simultaneous and continuous formations followed by deamination of $(NH_4)_2Zn(SO_4)_2$ and $(NH_4)_3Fe(SO_4)_3$ [40], and the formations of $CaSO_4$ and $PbSO_4$. Li et al. studied the decomposition process of $(NH_4)_2SO_4$ in detail, and presented the TG-DTA curves and the FT-IR spectra. The results showed that a large amount of NH_3 released at 384ºC and a large amount of SO_2 and H_2O produced at 520ºC [39]. Zhang et al. displayed the coincident TG-DTA curves obtained in argon protection and Yin et al. presented the homologous FT-IR spectra, and the most significant weight loss occurs at the temperature range of 450-520ºC due to the total decomposition of $(NH_4)_2SO_4$ (Eq. 3) [38, 41]. Yin et al. also pointed out that the decomposition of ammonium bisulfate was more difficult than that of $(NH_4)_2SO_4$ and the reaction rate of ammonium bisulfate with blast furnace slag was extremely fast

[41]. The chemical reactions mainly occurred before the total decomposition of $(NH_4)_2SO_4$ may be deduced as below.

$$ZnCO_3+2NH_4HSO_4 \rightarrow (NH_4)_2Zn(SO_4)_2+H_2O+CO_2 \quad (4)$$

$$Fe_2O_3+6NH_4HSO_4 \rightarrow 2(NH_4)_3Fe(SO_4)_3+3H_2O \quad (5)$$

$$(NH_4)_2Zn(SO_4)_2 \rightarrow ZnSO_4+2NH_3+H_2O+SO_3 \quad (6)$$

$$(NH_4)_3Fe(SO_4)_3 \rightarrow NH_4Fe(SO_4)_2+(NH_4)_2SO_4 \quad (7)$$

$$2NH_4Fe(SO_4)_2 \rightarrow Fe_2(SO_4)_3+(NH_4)_2SO_4 \quad (8)$$

$$CaCO_3+NH_4HSO_4 \rightarrow CaSO_4+NH_3+H_2O+CO_2 \quad (9)$$

$$PbCO_3+NH_4HSO_4 \rightarrow PbSO_4+NH_3+H_2O+CO_2 \quad (10)$$

3.2.5. Mechanism analysis

As discussed above, $(NH_4)_2SO_4$ was decomposed into NH_3 and NH_4HSO_4 before the total decomposition occurred at the temperature range of 350-450ºC. The reaction was a gas-liquid-solid reaction, thus, the shrinking unreacted core model was not suitable for the kinetic analysis. Another method, called the constant conversion method was adopted, as shown in Eq. (11) [41].

$$\ln(1/t) = \ln A - E_\alpha / RT \quad (11)$$

where t is the reaction time, min; A is frequency factor, min^{-1}; E_α is the apparent activation energy, $kJ \cdot mol^{-1}$.

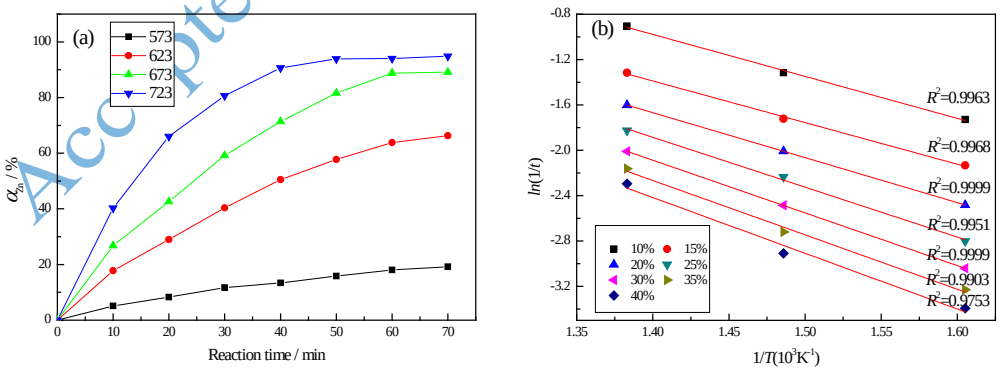

Fig. 6. (a) Relationships between holding time, temperature and extraction efficiency of Zn. (b) Plot of ln(1/*t*) versus 1/*T*.

The results plotted in Fig. 6(a) show that with the roasting temperature and time

rising, the extraction efficiency of Zn increases gradually. The roasting mechanism was discussed within 623 K to 723 K and the plot of ln(1/*t*) versus 1/*T* was shown in Fig. 6(b). The calculated value of the apparent activation energy from the slopes of those fitting lines is 41.74 kJ·mol^{-1}, which is in the typical range of chemical reaction control mechanism [43].

3.3. Water leaching mechanism

The investigation for the effects of leaching temperature, time, stirring velocity, L/S ratio on the leaching ratio of Zn was conducted and the results were plotted in Fig. 7.

3.3.1. Effect of temperature

The experiments for the influence of leaching temperature ranging from 20ºC to 95ºC were performed at conditions of L/S=4ml:1g, t=60 min and stirring velocity 400 r·min^{-1}. The leaching ratio of Zn increases with temperature rising (Fig. 7(a)). Increasing temperature enhances the dissolution of $ZnSO_4$ due to the improvement of molecular movement. After 90ºC, the Zn dissolution begins to decline slightly. This is attributed to the synthesis of ammonium jarosite, entraining Zn^{2+} as inclusion [44].

3.3.2. Effect of time

The study for the effect of leaching time was performed at conditions of L/S=4ml:1g, 90ºC and 400 r·min^{-1}. Prolonging leaching time increases the leaching efficiency of zinc within 60 min (Fig. 7(b)). But the increase is slight over 50 min. The following experiments were carried out at 50 min.

3.3.3. Effect of stirring velocity

The stirring velocity experiments ranging from 100 to 600 r·min^{-1} were completed at conditions of L/S=4ml:1g, 90ºC and 50 min. The Zn leaching ratio increases obviously with stirring velocity ranging from 100 r·min^{-1} to 400 r·min^{-1} (Fig. 7(c)), due to the improvement of relative motion of liquid-solid and the enhancement of mass transfer. But the change is slight when the stirring velocity varies from 400 to 600 r·min^{-1}, indicating that the effect of stirring velocity is relative weak. Thus, 400 r·min^{-1} was selected in following experiments.

3.3.4. Effect of L/S ratio

The impact of L/S ratio on zinc leaching ratio was studied at 90ºC and stirring for

50 min at 400 r·min^{-1}. The results plotted in Fig. 7(d) indicate that the Zn leaching ratio increases with L/S ratio rising within 4:1 because of the decrease of the ions concentration in water. Afterwards, the leaching ratio of Zn tends to be stable. Therefore, L/S ratio 4:1 was chosen.

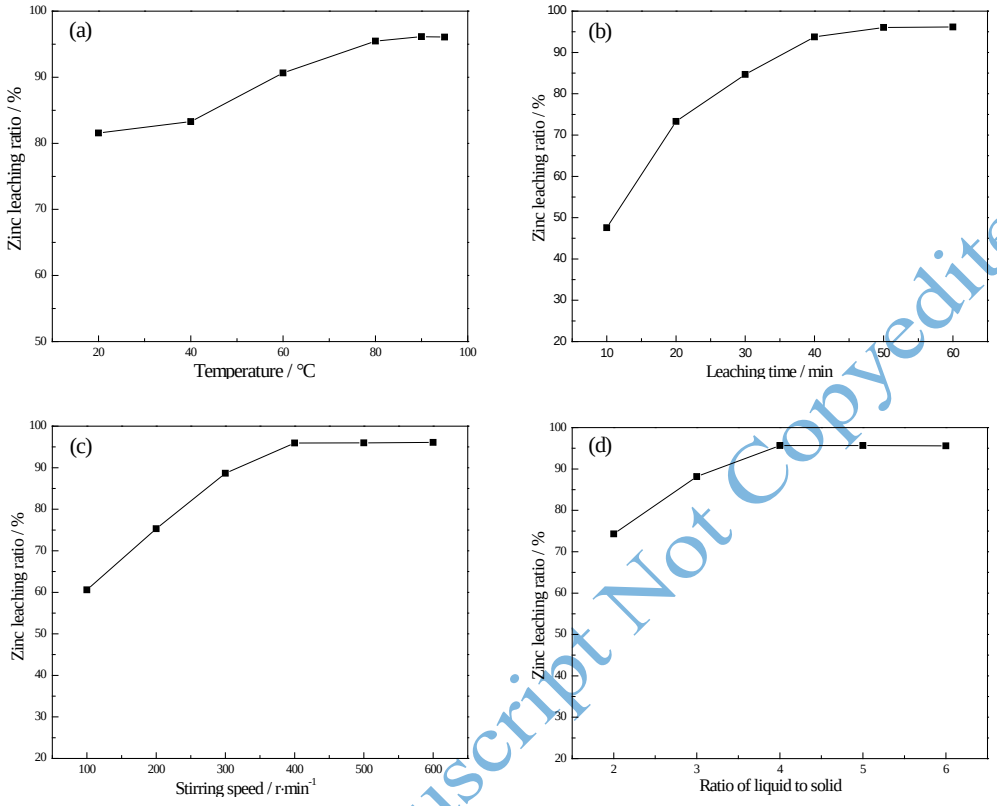

Fig. 7. Influence of (a) leaching temperature [L/S=4, 60 min, 400 r·min^{-1}]; (b) leaching time [L/S=4, 90°C, 400 r·min^{-1}]; (c) stirring velocity [L/S=4, 90°C, 50 min]; (d) L/S ratio [90°C, 50 min, 400 r·min^{-1}] on Zn dissolution ratio.

3.3.5. Kinetic investigation

The leaching efficiency of Zn with the leaching temperature (313 K-353 K) and time (0-60 min) was examined and plotted in Fig. 8(a). The leaching efficiency of Zn increases steadily with both temperature and time rising. Approximate 93% Zn is leached at 353 K over 40 min. The water leaching process is a typical liquid-solid reaction without solid product layer formation, so the following shrinking core model (Eq. (12)) is used to explain the kinetic mechanism.

$$1-(1-\alpha)^{2/3} = kt \tag{12}$$

where α is the reaction fraction, %; t is the reaction time, min.

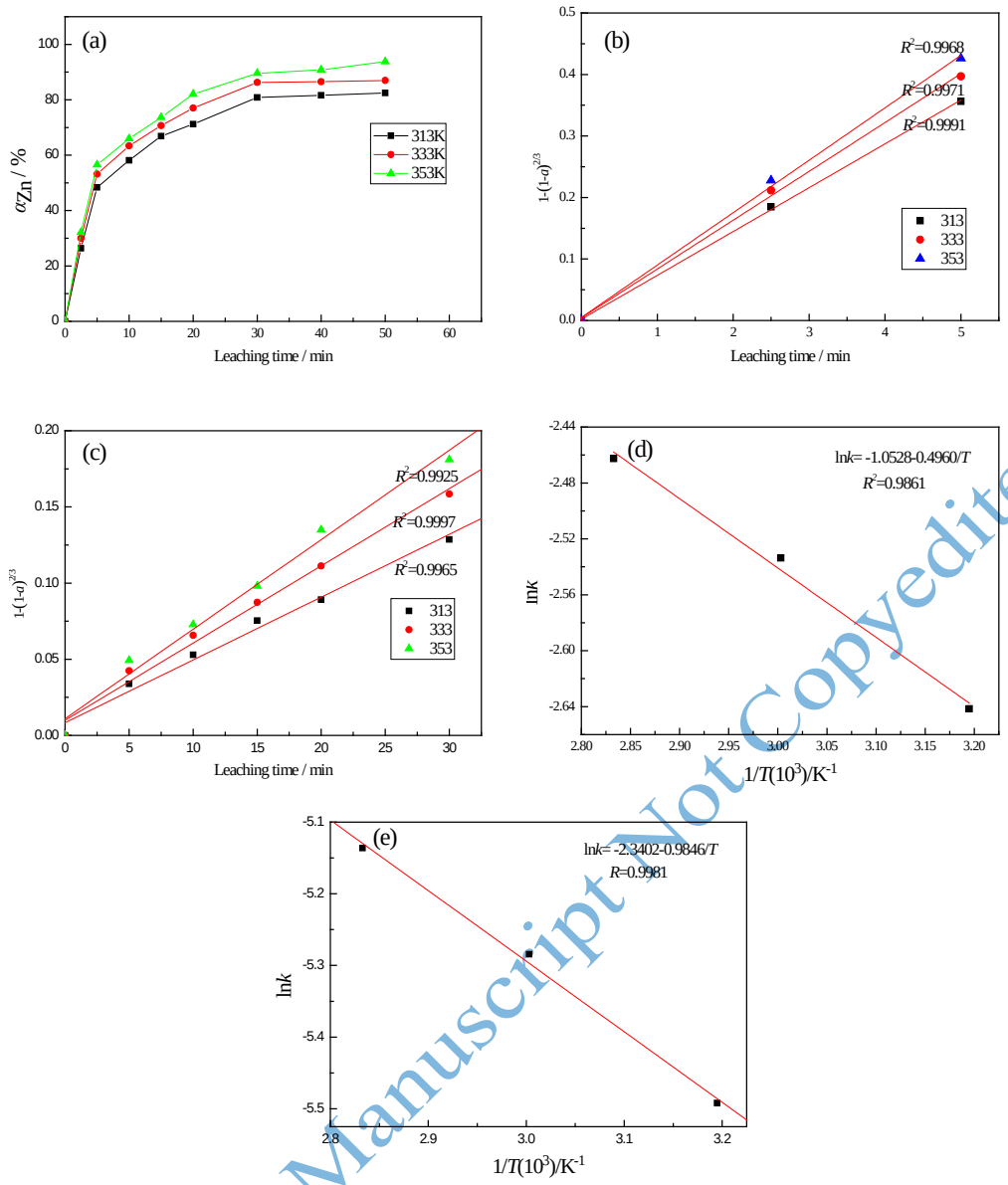

Fig. 8. (a) Variation of Zn leaching efficiency with leaching temperature and time. (b)and (c) Plots of 1-(1-α)$^{2/3}$ against t at different temperatures. (d) and (e) Plots of ln$k$ versus T^{-1}.

The leaching process can be divided into two stages of 0-5 min and 5-30 min. The kinetic data in Fig. 8(b) (0-5 min) and Fig. 8(c) (5-30min) is well agreement with Eq. (12). The Arrhenius plots of ln$k$ versus 1/T are presented in Fig. 8(d) and (e). The activation energy and pre-exponential factor can be calculated and the values are 4.12 kJ·mol^{-1} and 0.3490 min^{-1} for the first stage and 8.19 kJ·mol^{-1} and 0.0963 min^{-1} for the second stage, respectively. Thus, the reaction rate equation is presented as below.

$$1-(1-\alpha)^{2/3} = 0.3490\exp(-4{,}120/RT)t \quad (13)$$

$$1-(1-\alpha)^{2/3} = 0.0963\exp(-8{,}190/RT)t \quad (14)$$

3.4. Characterization of leaching residue

The main compositions in residue analyzed by chemical method are listed in Table 2. The contents of ZnO, Fe_2O_3 and SiO_2 are 1.94%, 12.02% and 51.82%, respectively. The PbO and SrO are enriched to 6.81% and 3.38%, respectively. The leaching residue is a valuable resource bearing Pb and Sr, which is worth to utilize rationally. The XRD pattern and SEM micrograph presented in Fig. 9 indicate that the main phases in residue are SiO_2, $PbSO_4$, $SrSO_4$, Fe_3O_4 and $CaSO_4$. The residue particles are irregular with rough surface.

Table 2. Main chemical compositions in leaching residue **wt/%**

Components	ZnO	Fe_2O_3	SiO_2	PbO	SrO	CaO
Content / wt%	1.94	12.02	51.82	6.81	3.38	4.67

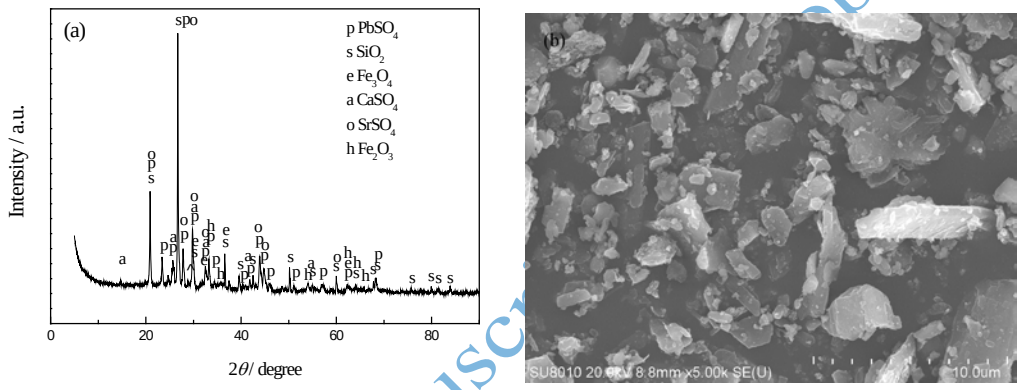

Fig. 9. (a) XRD pattern and (b) SEM micrograph of the residue.

4. Conclusions

(1) The effects of roasting and leaching parameters on zinc extraction were evaluated. Under operating conditions of molar ratio of $(NH_4)_2SO_4$ to zinc 1.4:1, roasting temperature 450ºC, holding time 1 h, leaching temperature 90ºC, time 50 min, stirring velocity 400 r·min^{-1} and L/S ratio 4:1, the extraction ratio of Zn reaches the maximun of 96%.

(2) Kinetic study demonstrates that the roasting process follows the chemical reaction control mechanism with the apparent activation energy value of 41.74 kJ·mol^{-1}. The leaching control step is the outer diffusion of no product layer with the apparent activation energy values of 4.12 kJ·mol^{-1} and 8.19 kJ·mol^{-1} for two stages.

(3) Ammonium sulfate roasting followed by water leaching can be adopted to

extract zinc from zinc oxidized ore and is effective in practice. $(NH_4)_2SO_4$ can be cyclic utilized in the whole process. It may be a potentially alternative method in dealing with zinc oxidized ore.

Acknowledgements

This work was financially supported by the National Natural Science Foundation of China (Grant Nos. 51774070, 51574084 and 51204054), and the National Key Research and Development Program of China (Grant No. 2017YFB0305401).

References

[1]. S.M.C. Santos, R.M. Machado, M.J.N. Correia, M.T.A. Reis, M.R.C. Ismael, and J.M.R. Carvalho, Ferric sulphate/chloride leaching of zinc and minor elements from a sphalerite concentrate, *Miner. Eng*., 23(2010), No. 8, p. 606-615.

[2]. Z.Y. Ding, Z.L. Yin, X.F. Wu, H.P. Hu, and Q.Y. Chen, Leaching kinetics of willemite in ammonia-ammonium chloride solution, *Metall. Mater. Trans. B.*, 42(2011), No. 4, p. 633-641.

[3]. Z.Y. Ding, Q.Y. Chen, Z.L. Yin, and K. Liu, Predominance diagrams for Zn(II)-NH_3-Cl^-- H_2O system, *T. Nonferr. Metal. Soc.*, 23(2013), No. 3, p. 832-840.

[4]. C.X. Li, H.S. Xu, Z.G. Deng, X.B. Li, M.T. Li, and C. Wei, Pressure leaching of zinc silicate ore in sulfuric acid medium, *T. Nonferr. Metal. Soc.*, 20(2010), No. 5, p. 918-923.

[5]. V. Safari, G. Arzpeyma, F. Rashchi, and N. Mostoufi, A shrinking particle-shrinking core model for leaching of a zinc ore containing silica, *Int. J. Miner. Process.*, 93(2009), No. 1, p. 79- 83.

[6]. S. Rao, D.C. Zhang, T.Z. Yang, W.F. Liu, L. Chen, H.B. Ling, and X.W. Zhang, Selective extraction of zinc from refractory hemimorphite using iminodiacetic acid as a complexing agent, *Jom-Us*, 69(2017), No. 10, p. 1909-1913.

[7]. L.Y. Feng, X.W. Yang, Q.F. Shen, M.L. Xu, and B.J. Jin, Pelletizing and alkaline leaching of powdery low grade zinc oxide ores, *Hydrometallurgy*, 89(2007), No. 3-4, p. 305-310.

[8]. Y. Li, J.K. Wang, W. Chang, C.X. Liu, J.B. Jiang, and F. Wang, Sulfidation roasting of low grade lead-zinc oxide ore with elemental sulfur, *Miner. Eng.*, 23(2010), No. 7, p. 563-566.

[9]. S.H. Yang, H. Li, Y.W. Sun, Y.M. Chen, C.B. Tang, and J. He, Leaching kinetics of zinc silicate in ammonium chloride solution, *T. Nonferr. Metal. Soc.*, 26(2016), No. 6, p. 1688-1695.

[10]. H.M. Shao, X.Y. Shen, Y. Sun, Y. Liu, and Y.C. Zhai, Reaction condition optimization and kinetic investigation of roasting zinc oxide ore using $(NH_4)_2SO_4$, *Int. J. Miner. Metall. Mater.*, 23(2016), No. 10, p. 1133-1140.

[11]. X.Y. Shen, H.M. Shao, H.M. Gu, B. Chen, Y.C. Zhai, and P.H. Ma, Reaction mechanism analysis of roasting Zn_2SiO_4 using NaOH, *T. Nonferr. Metal. Soc.*, 28(2018), No. 9, p. 1878-1886.

[12]. Z.L. Yin, Z.Y. Ding, H.P. Hu, K. Liu, and Q.Y. Chen, Dissolution of zinc silicate (hemimorphite) with ammonia-ammonium chloride solution, *Hydrometallurgy*, 103(2010), No. 1-4, p. 215- 220.

[13]. B. Chen, X.Y. Shen, H.M. Gu, H.M. Shao, Y.C. Zhai, and P.H. Ma, Extracting reaction mechanism analysis of Zn and Si from zinc oxide ore by NaOH roasting method, *J. Cent. South Univ.*, 24(2017), No. 10, p. 2266-2274.

[14]. S.M. He, J.K. Wang, and J.F. Yan, Pressure leaching of synthetic zinc silicate in sulfuric acid medium, *Hydrometallurgy*, 108(2011), No. 3-4, p. 171-176.

[15]. Y. Hua, Z. Lin, and Z. Yan, Application of microwave irradiation to quick leach of zinc silicate ore, *Miner. Eng.*, 15(2002), p. 451-456.

[16]. Y.C. Zhang, J.X. Deng, J. Chen, R.B. Yu, and X.R. Xing, Leaching of zinc from calcined smithsonite using sodium hydroxide, *Hydrometallurgy*, 131(2011), p. 89-92.

[17]. Y. Sun, X.Y. Shen, and Y.C. Zhai, Thermodynamics and kinetics of extracting zinc from zinc oxide ore by ammonium sulfate roasting method, *Int. J. Miner. Metall. Mater.*, 22(2015), No. 5, p. 467-475.

[18]. X.B. Min, K. Xue, Y. Ke, B.S. Zhou, Y.W.J. Li, and Q.W. Wang, Sulfidation Roasting of Hemimorphite with Pyrite for the Enrichment of Zn and Pb, *Jom-Us*, 68(2016), No. 9, p. 2435-2442.

[19]. S. Moradi, and A.J. Monhemius, Mixed sulphide oxide lead and zinc ores problems and solutions, *Miner. Eng.*, 24(2011), No. 10, p. 1062-1076.

[20]. Z.W. Zhao, S. Long, A.L. Chen, G.S. Huo, H.G. Li, X.J. Jia, and X.Y. Chen,

Mechanochemical leaching of refractory zinc silicate (hemimorphite) in alkaline solution, *Hydrometallurgy*, 99(2009), No. 3-4, p. 255-258.

[21]. W.Q. Qin, W.Z. Li, Z.Y. Lan, and G.Z. Qiu, Simulated small-scale pilot plant heap leaching of low-grade oxide zinc ore with integrated selective extraction of zinc, *Miner. Eng.*, 20(2007), No. 7, p. 694-700.

[22]. M.K. Jha, V. Kumar, and R.J. Singh, Review of hydrometallurgical recovery of zinc from industrial wastes, *Resour. Conserv. Recy.*, 33(2001), No. 1, p. 1-22.

[23]. H.S. Xu, C. Wei, C.X. Li, G. Fan, Z.G. Deng, M.T. Li, and X.B. Li, Sulfuric acid leaching of zinc silicate ore under pressure, *Hydrometallurgy*, 105(2010), No. 1-2, p. 186-190.

[24]. S.M. He, J.K. Wang, and J.F. Yan, Pressure leaching of high silica Pb-Zn oxide ore in sulfuric acid medium, *Hydrometallurgy*, 104(2010), No. 2, p. 235-240.

[25]. I.G. Matthew, and D. Elsner, The hydrometallurgical treatment of zinc silicate ores, *Metall. Mater. Trans. B.*, 8(1977), No. 1, p. 73-83.

[26]. Z.Y. Ding, Z.L. Yin, H.P. Hu, and Q.Y. Chen, Dissolution kinetics of zinc silicate (hemimorphite) in ammoniacal solution, *Hydrometallurgy*, 104(2010), No. 2, p. 201-206.

[27]. S. Espiari, F. Rashchi, and S.K. Sadrnezhad, Hydrometallurgical treatment of tailings with high zinc content, *Hydrometallurgy*, 82(2006), No. 1-2, p. 54-62.

[28]. A.C. Dou, T.Z. Yang, J.X. Yang, J.H. Wu, and A. Wang, Leaching of low grade zinc oxide ores in Ida(2)-H_2O system, *T. Nonfer. Metal. Soc.*, 21(2011), No. 11, p. 2548-2553.

[29]. A.L. Chen, M.C. Li, Z. Qian, Y.T. Ma, J.Y. Che, and Y.L. Ma, Hemimorphite ores: a review of processing technologies for zinc extraction, *Jom-Us*, 68(2016), No. 10, p. 2688-2697.

[30]. A.L. Chen, Z.W. Zhao, X.J. Jia, S. Long, G.S. Huo, and X.Y. Chen, Alkaline leaching Zn and its concomitant metals from refractory hemimorphite zinc oxide ore, *Hydrometallurgy*, 97(2009), No. 3-4, p. 228-232.

[31]. E. Abkhoshk, E. Jorjani, M.S. Al-Harhsheh, F. Rashchi, and M. Naazeri, Review of the hydrometallurgical processing of non-sulfide zinc ores, *Hydrometallurgy*, 149(2014), p. 153-167.

[32]. Q. Liu, T.C. Zhao, and G.D. Zhao, Production of zinc and lead concentrates from lean oxidized zinc ores by alkaline leaching followed by two-step precipitation using sulfides, *Hydrometallurgy*, 110(2011), No. 1-4, p. 79-84.

[33]. S.M. Mousavi, S. Yaghmaei, M. Vossoughi, A. Jafari, and R. Roostaazad, Zinc extraction from Iranian low-grade complex zinc-lead ore by two native microorganisms: Acidithiobacillus ferrooxidans and Sulfobacillus, *Int. J. Miner. Process.*, 80(2006), No. 2-4, p. 238-243.

[34]. X.L. Xu, W.Z. Liu, G.R. Chu, G.Q. Zhang, D.M. Luo, H.R. Yue, B. Liang, and C. Li, Energy-efficient mineral carbonation of $CaSO_4$ derived from wollastonite via a roasting-leaching route, *Hydrometallurgy*, 184(2019), p. 151-161.

[35]. J.P. Hu, W.Z. Liu, L. Wang, Q. Liu, F. Chen, H.R. Yue, B. Liang, L. Lü, Y. Wang, G.Q. Zhang, and C. Li, Indirect mineral carbonation of blast furnace slag with $(NH_4)_2SO_4$ as a recyclable extractant, *J. Energy Chem.*, 26(2017), p. 927-935.

[36]. L. Wang, W.Z. Liu, J.P. Hu, Q. Liu, H.R. Yue, B. Liang, G.Q. Zhang, D.M. Luo, H.P. Xie, and C. Li, Indirect mineral carbonation of titanium-bearing blast furnace slag coupled with recovery of TiO_2 and Al_2O_3, Chinese J. Chem. Eng., 26(2018), p. 583-592.

[37]. W.Z. Liu, X.M. Wang, Z.P. Lu, H.R. Yue, B. Liang, L. Lü, and C. Li, Preparation of synthetic rutile via selective sulfation of ilmenite with $(NH_4)_2SO_4$ followed by targeted removal of impurities, Chinese J. Chem. Eng., 25(2017), p. 821-828.

[38]. G.Q. Zhang, D.M. Luo, C.H. Deng, L. Lv, B. Liang, C. Li, Simultaneous extraction of vanadium and titanium from vanadium slag using ammonium sulfate roasting-leaching process, *J. Alloy. Compd.*, 742(2018), p. 504-511.

[39]. Y.C. Li, H. Liu, B. Peng, X.B. Min, M. Hu, N. Peng, Y.Z. Yuang, J. Lei, Study on separating of zinc and iron from zinc leaching residues by roasting with ammonium sulphate, *Hydrometallurgy*, 158(2015), p. 42-48.

[40]. W.N. Mu, F.H. Cui, Z.P. Huang, Y.C. Zhai, Q. Xu, S.H. Shao, Synchronous extraction of nickel and copper from a mixed oxide-sulfide nickel ore in a low-temperature roasting system, *J. Clean. Prod.*, 177(2018), p. 371-377.

[41]. S. Yin, T. Aldahri, S. Rohani, C. Li, D.M. Luo, G.Q. Zhang, H.R. Yue, B. Liang, W.Z. Liu, Insights into the roasting kinetics and mechanism of blast furnace slag with ammonium sulfate for CO_2 mineralization, *Ind. Eng. Chem. Res.*, 58(2019), No. 31, p. 14026-14036.

[42]. W.Z. Liu, S. Yin, D.M. Luo, G.Q. Zhang, H.R. Yue, B. Liang, L.M. Wang, and C. Li, Optimising the recovery of high-value-added ammonium alum during mineral carbonation of

blast furnace slag, *J. Alloy. Compd.*, 774(2019), p. 1151-1159.

[43]. Y.X. Hua, *Introduction of Metallurgical Process Kinetics*, 1st Ed, Metallurgical Industry Press, Beijing, 2004. (in Chinese)

[44]. H.M. Shao, X.Y. Shen, B.B. Zhang, and Y.C. Zhai, Purification of the digestion solution of zinc oxide ores, *J. Northeast Univ.*, 36(2015), No. 6, p. 811-814. (in Chinese)

中图分类号：**TF813**　　二级学科：冶金物理化学

Chinese Library Classification: **TF813**　　Second Disciplines: Physical Chemistry of Metallurgy